

## Article

# A Method of Reducing Friction and Improving the Penetration Rate by Safely Vibrating the Drill-String at Surface

Yuan Long <sup>1,2,3</sup>, Xueying Wang <sup>1,2,3,\*</sup> , Peng Wang <sup>4</sup> and Feifei Zhang <sup>1,2,3</sup><sup>1</sup> School of Petroleum Engineering, Yangtze University, Wuhan 430100, China<sup>2</sup> National Engineering Research Center for Oil & Gas Drilling and Completion Technology, Yangtze University, Wuhan 430100, China<sup>3</sup> Hubei Key Laboratory of Oil and Gas Drilling and Production Engineering, Yangtze University, Wuhan 430100, China<sup>4</sup> School of Petroleum Engineering, China University of Petroleum (East China), Qingdao 266580, China

\* Correspondence: wangxy@yangtzeu.edu.cn

**Abstract:** Drill-string axial vibration at the surface technology is proposed to reduce the friction between the drill-string and the borehole wall, and to improve load transfer efficiency, the rate of penetration (ROP), and the extended-reach limit of a horizontal well. An analytical framework utilizing the “soft-string” model is constructed. The results obtained from numerical simulations reveal that during the slide drilling operation, the drill-string experiences an axial stick–slip motion, and the weight on bit (WOB) undergoes periodic oscillations. The conventional calibration method of the WOB in the weight indicator gauge is not applicable when the ROP is low. After applying axial vibration on the drill-string at the surface, the WOB increases and becomes smooth because of a release of friction. The amplitude and frequency of the exciting force are the main factors affecting surface vibration effectiveness. There is an optimal frequency for a given case (10 Hz in this paper). This means that the conventional manual pick-up and slack-off by drillers with a high amplitude and a low frequency has little effect on friction reduction. In addition, the conventional method can bring in high risk because of its high root mean square (RMS) acceleration. Safety evaluation results indicate that the drill-string is in a safe state under most of the exciting parameters. The results verify the feasibility and advantages of the proposed technology, and lay a solid theoretical foundation for its application in real drilling applications.

**Keywords:** petroleum drilling; drill-string mechanics; friction reduction; vibration

**Citation:** Long, Y.; Wang, X.; Wang, P.; Zhang, F. A Method of Reducing Friction and Improving the Penetration Rate by Safely Vibrating the Drill-String at Surface. *Processes* **2023**, *11*, 1242. <https://doi.org/10.3390/pr11041242>

Academic Editors: Tianshou Ma and Yuqiang Xu

Received: 19 March 2023

Revised: 7 April 2023

Accepted: 14 April 2023

Published: 17 April 2023



**Copyright:** © 2023 by the authors. Licensee MDPI, Basel, Switzerland. This article is an open access article distributed under the terms and conditions of the Creative Commons Attribution (CC BY) license (<https://creativecommons.org/licenses/by/4.0/>).

## 1. Introduction

Drilling complex structural wells (such as directional, horizontal, and extended reach wells) is essential for the successful exploitation of petroleum and natural gas reserves. These types of wells ensure optimal formation exposure and increase the chances of hitting the pay zone. Moreover, these wells are suitable for future stimulation techniques, which can significantly improve well production efficiency and final recovery rates. Directional drilling realized by combining a positive displacement motor (PDM) and measurement while drilling (MWD), which is known as slide drilling, is an effective well trajectory control method and is widely used worldwide. This technology has its drawbacks, as the lack of rotation in the drill-string creates significant friction with the borehole wall. As a result, the transfer of axial load to the bit decreases, leading to a reduction in both the rate of penetration (ROP) and the extended-reach limit. Meanwhile, the stick–slip phenomenon of the drill-string is further intensified by the frequent transform between static and dynamic friction force. Reducing the amount of resistance between the drill-string and the borehole wall and enhancing the effectiveness of load transfer during directional drilling are essential objectives with significant importance in petroleum drilling that have been given attention for several years [1].

Two main approaches are typically employed in friction reduction research, namely reducing the normal contact force and decreasing the coefficient of friction. To decrease the normal contact force, one can optimize the well track and make use of a lightweight drill pipe. To reduce the friction coefficient, it is possible to develop a high-performance lubricant, utilize a cylindrical roller sub, and incorporate a nonrotating protective joint. Adding vibrators to the drill-string was first proposed by Roper in 1983 as a means of reducing friction between the drill-string and the borehole wall. Although categorized as passive methods of friction reduction, these techniques have limited effectiveness [2]. In the past, the concept of utilizing a vibrator for petroleum drilling technology was not extensively researched. However, in recent years, various technology service companies have started conducting application studies on this idea and concentrated their efforts towards enhancing the vibrator's development [3,4]. Axial vibration friction reduction tools were first developed and widely used, represented by Agitator of National Oilwell Varco [5,6]. Then lateral vibration friction reduction tools were developed, represented by Xcite. The research concluded that axial vibration tools provide significantly more effective friction reduction in horizontal wells [7]. Axial and lateral vibration friction reduction patterns are realized by adding downhole tools in the drill-string, which will consume hydraulic energy. Moreover, drillers need to trip out and reassemble the makeup of the string when the well depth goes to a deeper extent. Contrary to the aforementioned vibration technologies, the automatic surface rocking technology utilizes the top drive to rotate the drill-string to the right limit and then to the left limit by a predetermined amount, without relying on any downhole tool. This innovative technique is exemplified by the "Slider" [8] and "DSCS" [9] systems. However, it is sometimes difficult to control the real-time toolface orientation because of dynamic reactive torque from bit-rock interaction.

After weighing the pros and cons of the aforementioned vibration methods, our proposition is to apply axial vibration on the drill-string at the surface. This will reduce the friction between the drill-string and the borehole wall while enhancing the efficiency of load transfer. The excitation means may be displacement or force. Compared to other exciting manners (such as the axial vibration tool Agitator, the lateral vibration tool Xcite, and the torsional vibration system Slider), the technology of drill-string axial vibration at the surface proposed in this paper has the following advantages: Firstly, no drilling fluid energy is needed for vibrating the drill-string, which make it feasible to use and suited for a deep well. Secondly, exciting parameters are adjustable at any time according to the real-time drilling situation through simple surface tools. Thirdly, key seating and pressure differential sticking can also be overcome by applying a higher amplitude and lower frequency excitation.

Scholars have developed many torque and drag calculation models in the last decades, which can be divided into soft-string models [10–14] and stiff-string models [15–18]. However, these models can only be used for calculating the drag while tripping in or tripping out, and the torque while rotating drilling. When the drill-string is vibrated axially at the surface, the drill-string elements are frequently in the states of forward sliding, resting, and backward sliding, which makes the above models not applicable. Meanwhile, dynamic models [19] can be used to study the motion and force characteristics along the whole drill-string, and the load transfer efficiency can be obtained based on the deformation of the drill-string. However, these dynamic models usually focus on the rotating drilling mode, and neglect the axial friction or assume it as linear viscous damping. The study of friction reduction and load transfer in drill-strings under vibrational conditions is significantly lagging behind the advancements made in friction reduction technologies through the applications of vibrating drill-strings. Several scholars have devised models for determining the load transfer of a drill-string subjected to vibration [20–23]. However, the friction model in these models is the Coulomb model that does not consider the viscous effect of friction. The research on the mechanism of friction reduction by applying vibration can provide a reference for choosing a friction model [24]. The friction reduction mechanisms of vibration mainly include: (a) the static friction transforms to dynamic friction due to

axial and torsional vibrations [6]; (b) during the cycle of vibration, the direction of dynamic friction is altered by both axial and torsional vibrations, leading to a reduction in the mean friction force [25,26]; and (c) the lateral vibration decreases the normal contact force periodically [27]. Based on these mechanisms, under vibration conditions, the dynamic friction models that take pre-slip displacement into account are better choices to simulate drill-string dynamics.

In this paper, the load transfer characteristics of the drill-string while being vibrated axially at the surface is studied. Firstly, friction is incorporated based on the pre-slip displacement of the drill-string to accurately calculate the friction distribution of the whole drill-string during its axial vibration. The dynamic friction model is used to capture the change in coefficient and a basic model is derived according to the equilibrium of forces. The established numerical model is solved using a finite difference method. Subsequently, evaluations of the load transfer characteristics of the drill-string under both displacement and force excitations are conducted and compared with other types of vibration patterns. The main objective of this study is to demonstrate the viability and benefits of a new technique, which involves axial vibration at the surface to reduce friction. By comparing its load transfer properties with other types of vibration, we aim to establish a strong theoretical basis for the application of this technology in actual drilling.

## 2. Model

### 2.1. Assumptions

The drill-string undergoes a complex motion (rolling, revolution, and swirling) and deformation (bending, sinusoidal buckling, and helical buckling) due to the intricate forces exerted on it while drilling underground. In the process of directional drilling, the drill-string remains stationary and experiences significant resistance and drag from the borehole wall. As a result, both rotational and lateral movements are negligible, while axial movement becomes the primary motion. The resistance and drag also decrease the likelihood of buckling occurring, particularly in horizontal sections [28]. The main focus of this study is to examine how axial excitation impacts the load transfer in the directional drilling process of a structurally complex well. Therefore, the following assumptions are made:

- (a) Assuming there is no clearance between the drill-string and the borehole wall, the centerline of the drill-string perfectly aligns with the centerline of the borehole, and the drill-string maintains consistent contact with the borehole wall.
- (b) Each vibrator is seen as a length of drill-string, and its exciting force is sinusoidal.
- (c) Friction and viscous damping of drilling fluid are the two main types of damping forces acting on the drill-string, while mechanical resistance caused by key seating and differential pressure sticking are excluded from consideration.
- (d) The analysis focuses on the axial dynamic impact of the drill-string, disregarding the cross-sectional forces of shear and bending moment.

### 2.2. Equilibrium Equation

To derive the dynamic equation for the vibration process of a drill-string, a small drill-string element  $ds$  is selected and analyzed. The element is considered in natural curvilinear coordinates  $(\vec{e}_t, \vec{e}_n, \vec{e}_b)$ , and is subjected to various forces, such as internal tension force  $\vec{T}$ , normal contact force  $\vec{F}$ , friction force  $F_f$ , damping force, and buoyant weight of drilling (as displayed in Figure 1). By balancing these forces, we can arrive at an equation that describes the dynamic equilibrium condition [29]:

$$\begin{aligned} \vec{T}(s+ds, t) - \vec{T}(s, t) + \vec{F}\left(s + \frac{ds}{2}, t\right) ds - [F_f(s, t) + c\left(s + \frac{ds}{2}, t\right) \frac{\partial u(s + \frac{ds}{2}, t)}{\partial t}] ds \vec{e}_t \\ + g_s\left(s + \frac{ds}{2}\right) ds \vec{e}_g = \rho\left(s + \frac{ds}{2}\right) A\left(s + \frac{ds}{2}\right) ds \frac{\partial^2 u(s + \frac{ds}{2}, t)}{\partial t^2} \vec{e}_t \end{aligned} \quad (1)$$

where  $T_t(s, t)$ ,  $T_n(s, t)$ , and  $T_b(s, t)$  are internal forces acting on cross-section in  $\vec{e}_t$ ,  $\vec{e}_n$ , and  $\vec{e}_b$  direction, respectively;  $F_n, F_b$  are the lateral contact force acting on drill-string in principal normal  $\vec{e}_n$  and binormal direction  $\vec{e}_b$ , respectively.

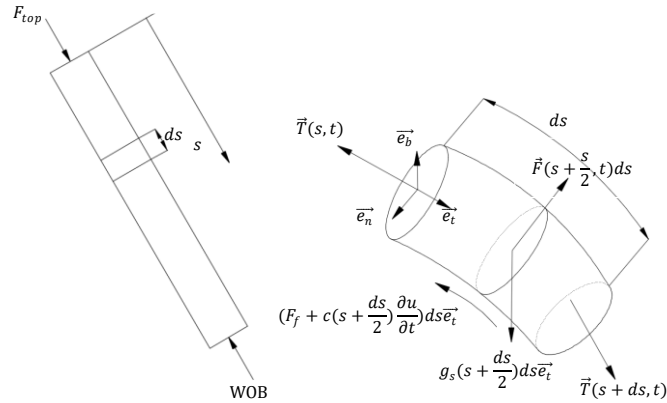


**Figure 1.** Forces acting on a drill-string element.

The following simpler equilibrium equation can be derived from the Taylor expansion in  $(s, t)$  of variables by omitting higher order terms:

$$\frac{\partial \vec{T}(s, t)}{\partial s} + \vec{F}(s, t) - [F_f(s, t) + c(s, t) \frac{\partial u}{\partial t}] \vec{e}_t + g_s(s) \vec{e}_g = \rho(s) A(s) \frac{\partial^2 u(s, t)}{\partial t^2} \vec{e}_t \quad (2)$$

Separating the internal force  $\vec{T}$  and distributed lateral contact force  $\vec{F}$  into components in natural curvilinear coordinates  $(\vec{e}_t, \vec{e}_n, \vec{e}_b)$ :

$$\vec{T}(s, t) = T_t(s, t) \vec{e}_t + T_n(s, t) \vec{e}_n + T_b(s, t) \vec{e}_b \quad (3)$$

$$\vec{F}(s, t) = F_n(s, t) \vec{e}_n + F_b(s, t) \vec{e}_b \quad (4)$$

where  $T_t(s, t), T_n(s, t)$ , and  $T_b(s, t)$  are internal forces acting on cross-section in  $\vec{e}_t, \vec{e}_n$ , and  $\vec{e}_b$  direction, respectively;  $F_n, F_b$  are the lateral contact forces acting on drill-string in principal normal  $\vec{e}_n$  and binormal direction  $\vec{e}_b$ , respectively.

The Frenet–Serret formulas can be used to describe the centerline of the borehole [15]:

$$\begin{aligned} \vec{e}_g \cdot \vec{e}_t &= \cos \bar{\alpha} \\ \vec{e}_g \cdot \vec{e}_n &= \frac{k_\alpha}{k_b} \sin \bar{\alpha} \\ \vec{e}_g \cdot \vec{e}_b &= -\frac{k_\varphi}{k_b} (\sin \bar{\alpha})^2 \\ \vec{e}_g &= -\cos \bar{\alpha} \vec{e}_t + \frac{k_\alpha}{k_b} \sin \bar{\alpha} \vec{e}_n + \frac{k_\varphi}{k_b} \sin^2 \bar{\alpha} \vec{e}_b \end{aligned} \quad (5)$$

where  $\alpha, \varphi$ , and  $\bar{\alpha}$  are inclination angle, azimuth angle, and mean inclination angle, respectively;  $k_\alpha, k_\varphi$ , and  $k_b$  are rate of change of inclination angle, rate of change of azimuth angle, and total bending curvature, respectively.

The following scalar equations can be obtained by substituting Equations (3)–(5) into Equation (2):

In  $\vec{e}_t$  direction:

$$\frac{\partial T_t}{\partial s} - F_f(s, t) - c \frac{\partial u}{\partial t} + g_s \cos \bar{\alpha} = \rho A \frac{\partial^2 u}{\partial t^2} \quad (6)$$

In  $\vec{e}_n$  direction:

$$F_n + T_t k_b + g_s \frac{k_\alpha}{k_b} \sin \alpha = 0 \quad (7)$$

In  $\vec{e}_b$  direction:

$$F_b + g_s \frac{k_\varphi}{k_b} (\sin \alpha)^2 = 0 \quad (8)$$

The internal tension force  $T_t$  in axial direction for a rod can be written in the following form:

$$T_t = EA \frac{\partial u}{\partial s} \quad (9)$$

where  $E$  is the elastic (Young's) modulus of drill-string.

The distributed lateral contact force between drill-string and borehole wall can be obtained by combining Equations (7) and (8):

$$F = \sqrt{F_n^2 + F_b^2} = \left[ \left( T k_b + g_s \frac{k_\alpha}{k_b} \sin \alpha \right)^2 + \left( g_s \frac{k_\varphi}{k_b} (\sin \alpha)^2 \right)^2 \right]^{\frac{1}{2}} \quad (10)$$

The friction force  $F_f$  is calculated by Dahl friction model [30], which has the following form:

$$\begin{cases} \frac{dz}{dt} = v_r \cdot \left[ 1 - \frac{K}{F_c} \cdot z \cdot \text{sgn}(v_r) \right]^i \\ F_f = K_t \cdot z \end{cases} \quad (11)$$

where  $F_f$  is the axial friction force;  $F_c$  is the Coulomb friction force,  $F_c = \mu_d \cdot F$ ,  $\mu_d$  is the dynamic sliding friction coefficient;  $K$  is the tangential stiffness of contact surfaces;  $i$  is the parameter that determines the shape of strain–stress curve, in general  $i = 1$ ;  $t$  is the time;  $z(t)$  is the offset displacement of asperities at time  $t$ ;  $v_r$  is the relative velocity of drill-string.

### 2.3. Boundary and Initial Conditions

#### 2.3.1. Boundary Condition

##### (a) Surface boundary

During the drilling process, drillers aim to control the hook load at surface in order to adjust the actual weight on bit (WOB) to the desired value. This is achieved by ensuring that the hook load, which is the difference between the buoyant weight of the drill-string in the axial direction and the friction force and nominal WOB, is equivalent to the desired value. The request for the driller to maintain a constant hook load results in the friction force and nominal WOB being viewed as constant values. This, however, is subject to change due to the heterogeneity of rocks and the stick–slip motion of the drill-string, which causes the friction force and nominal WOB to transform interchangeably. The zero WOB is determined by running downward the drill-string at constant speed and setting the pointer on the weight indicator to zero before the bit reaches bottom of the well. However, the ROP may be very small in drilling processes, and partial drill-string may be in static friction state. In this case, the real WOB may be very small. With that in mind, we adopt static friction of drill-string to calculate hook load. The hook load can be determined through an analysis of the drill-string under static conditions where the frictional coefficient is equal to the static friction coefficient and the nominal WOB remains constant throughout subsequent calculations.

$$F_{top} = \left( G_t - \text{WOB} - F_{f,s} \right) + F_a \sin(\omega t) \quad (12)$$

where  $F_{top}$  is the hook load;  $G_t$  is the axial component of gravity of the whole drill-string;  $F_{f,s}$  is the total static friction of drill-string;  $F_a$  is the amplitude of exciting force;  $\omega$  is the circular frequency of the excitation.

## (b) Bit boundary

Generally, a vibrator is typically only required when the ROP is low. Whether the ROP is high or low, the drill-string movement will inevitably experience a stick–slip phenomenon during the slide drilling process, which will cause fluctuations in WOB. Varying WOB will result in varying ROP, which in turn affects the WOB. In 1970, Amoco petroleum exploration and development corporation proposed binary drilling rate model according to a great field of data, and used different bit weight exponent and rotate speed exponent in different hardness stratum. When the stratum changes from soft to hard, bit weight exponent changes from small to big, and rotate speed exponent changes from big to small, and the variation trend of penetration rate changes from fast to slow. The drilling rate model has the following form [31]:

$$ROP = K \cdot WOB^a \cdot n^b = K' \cdot WOB^a \quad (13)$$

where  $n$  is bit rotate speed;  $a$  and  $b$  are WOB exponent and bit rotate speed exponent, respectively.

## 2.3.2. Initial Conditions

If we suppose that the drill-string starts from rest, with zero initial velocity. The initial position of the drill bit is set to zero, while the initial position of the remaining section of the drill-string can be determined through static force equilibrium calculations.

$$\left. \frac{\partial u}{\partial t} \right|_{t=0} = 0 \quad (14)$$

$$u|_{t=0} = \Phi(T_t), u(L)|_{t=0} = 0$$

where  $\Phi$  is a mapping function from the initial tension distribution to initial displacement distribution of the drill-string.

## 2.4. Solution Method

Essentially, the model described involves the propagation of elastic waves. To solve it, a finite difference method has been selected in this section. The governing differential equation has been dispersed using a central difference scheme. After this, the differential equations are converted into algebraic equations and solved using MATLAB programing.

To begin with, the drill-string is segmented into  $N$  sections, spanning from the top to the bottom of the well. Difference grids are formed while setting time step  $\tau$  and space step  $h$ . Subsequently, the node displacement of the drill-string is represented as  $u(p, k)$  where  $p$  and  $k$  represent the position and time, respectively, and are abbreviated as  $u(p \cdot h, k \cdot \tau)$ .

There is nonlinear term  $\frac{\partial(EA \frac{\partial u}{\partial s})}{\partial s}$  in the governing differential equation. In order to deal with this nonlinear preferably, the governing differential equation is integrated for random node  $p$  in interval  $[(p - \frac{1}{2})h, (p + \frac{1}{2})h]$ . We can obtain the following Equation [29]:

$$\begin{aligned} & \left( EA \frac{\partial u}{\partial s} \right)^{p+\frac{1}{2}} - \left( EA \frac{\partial u}{\partial s} \right)^{p-\frac{1}{2}} - \frac{u(p, k+1) - u(p, k-1)}{2\tau} \int_{(p-\frac{1}{2})h}^{(p+\frac{1}{2})h} cds + \int_{(p-\frac{1}{2})h}^{(p+\frac{1}{2})h} g_s \cos \bar{\alpha} ds \\ & - \text{sgn}(u(p, k) - u(p, k-1)) \int_{(p-\frac{1}{2})h}^{(p+\frac{1}{2})h} F \mu ds = \frac{u(p, k+1) - 2u(p, k) + u(p, k-1)}{\tau^2} \int_{(p-\frac{1}{2})h}^{(p+\frac{1}{2})h} \rho A ds \end{aligned} \quad (15)$$

where  $\text{sgn}()$  is the sign function;  $h$  is space size;  $\tau$  is time step.

We denote:

$$T^{p+\frac{1}{2}} = \left( EA \frac{\partial u}{\partial s} \right)^{p+\frac{1}{2}} = EA \frac{u(p+1, k) - u(p, k)}{h} \quad (16)$$

$$T^{p-\frac{1}{2}} = \left( EA \frac{\partial u}{\partial s} \right)^{p-\frac{1}{2}} = EA \frac{u(p, k) - u(p-1, k)}{h} \quad (17)$$

$$F_f(p, k) = \text{sgn}(u(p, k) - u(p, k - 1)) \int_{(p-\frac{1}{2})h}^{(p+\frac{1}{2})h} F_f \mu ds \quad (18)$$

$$C^p = \int_{(p-\frac{1}{2})h}^{(p+\frac{1}{2})h} cds \quad (19)$$

$$A^p = \int_{(p-\frac{1}{2})h}^{(p+\frac{1}{2})h} \rho A ds \quad (20)$$

$$g^p = \int_{(p-\frac{1}{2})h}^{(p+\frac{1}{2})h} g_s \cos \bar{\alpha} ds \quad (21)$$

Substitute Equations (16)–(21) into (15), we can obtain the recurrence algorithm of drill-string axial displacement:

$$u(p, k + 1) = \frac{2\tau^2}{2A^p + C^p\tau} \left[ T^{p+\frac{1}{2}} - T^{p-\frac{1}{2}} - F_f(p, k) + g^p + \frac{2A^p}{\tau^2} u(p, k) + \left( \frac{C^p\tau - 2A^p}{2\tau^2} \right) u(p, k - 1) \right] \quad (22)$$

Difference solution format (22) is explicit. If we know the displacement of two former time steps, we can calculate drill-string displacement at any time step, and then the drilling parameters, such as axial tension force and WOB, can be obtained.

In order to achieve convergence of the solution, there must be a specific relationship between the time step  $\tau$  and the space step  $h$ . By utilizing the Fourier error analysis method, it has been proven that the difference scheme of Equation (22) is only stable under certain conditions. This condition can be expressed as the convergence condition:

$$\tau \leq \frac{h}{\sqrt{\frac{E}{\rho}}} \quad (23)$$

### 3. Results and Discussion

#### 3.1. Advantages of Surface Vibrating Technology

Nominal WOB equals the vector sum of the hook load  $F_{top}$ , the gravity of the drill-string, the real WOB, and the static friction between the drill-string and the borehole in the axial direction of the drill-string. A nominal constant WOB is applied and we expect to obtain a constant real WOB and ROP in conventional slide drilling. However, the real WOB and ROP are variational because of the existence of friction between the drill-string and the borehole wall and the stick–slip motion of the drill-string. We choose a representative horizontal well to analyze its load transfer characteristics. The well profile is shown in Figure 2. The well depth is 4200 m, and the kickoff point and landing point are 1290 m and 2190 m, respectively, and the build-up rate is 0.0524 rad/30 m. The drill-string is made up of  $\varnothing 127$  mm drill pipe, whose inner diameter, density, and elasticity modulus are 108.6 mm, 7850 kg/cm<sup>3</sup>, and 210 GPa, respectively. Other calculating parameters are as follows: the static and dynamic frictional coefficient are equal to 0.3 and 0.25 (static coefficient is always 1.2 times of dynamic coefficient [6]), respectively. The time step is 0.00005 s and the space step is 5 m. The exchange critical velocity of static friction and dynamic friction is 0.01 m/s. A binary model of the ROP and the WOB is adopted (see Equation (13)), in which  $WOB_{cri} = 20$  kN,  $a = 1$ , and  $K' = 5 \times 10^{-5}$ . Under such circumstances, the static friction and dynamic friction of the whole drill-string are 173 kN and 144 kN, respectively. Therefore, the maximal friction released by vibration equals 29 kN. The increase in the WOB also includes the exciting force and inertia force of the drill-string.

Figure 3 shows the variations in the real WOB and ROP with a different nominal WOB. From Figure 3, although the nominal WOB applied at the surface is constant, the real WOB and ROP at the bottom are fluctuant because of the static–dynamic friction switch and

stick-slip. Moreover, the real WOB transmitted to the bit increases with the increase in the nominal WOB. The amplitude and frequency of real WOB fluctuation decrease with the increase in the nominal WOB because of the continuous and steady motion of the drill-string under a high nominal WOB.

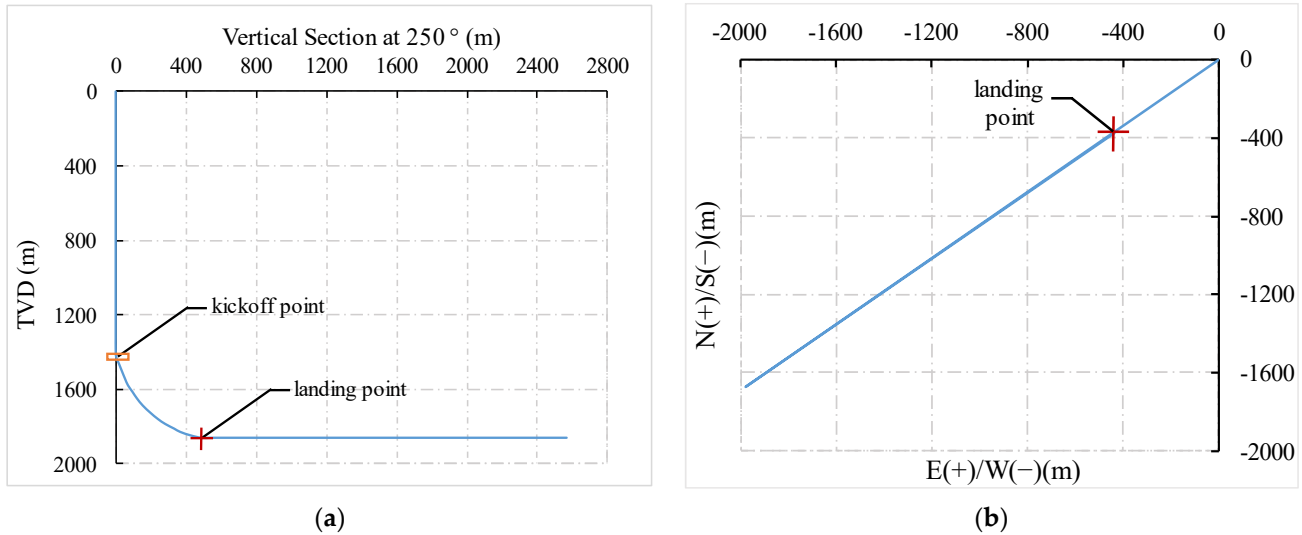


Figure 2. Well profile of a horizontal well. (a) Vertical projection view. (b) Horizontal projection view.

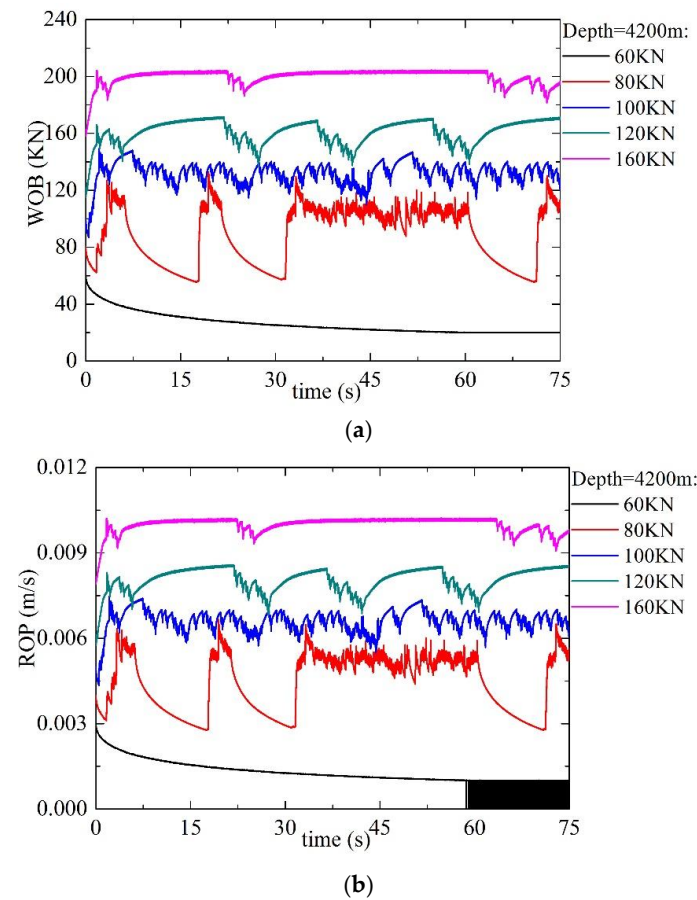
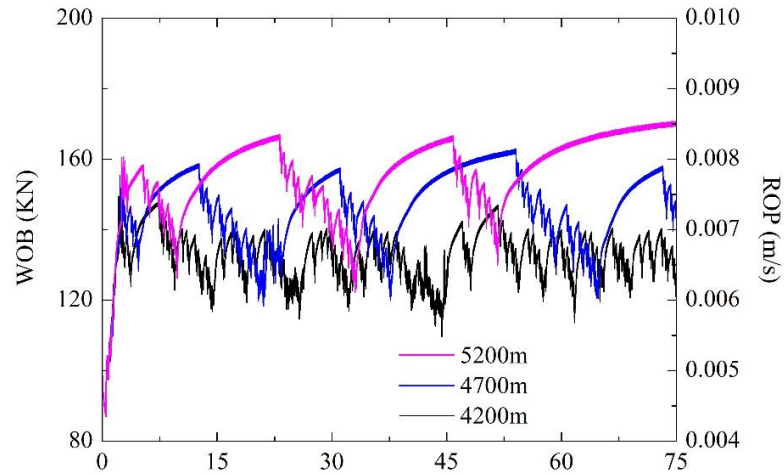


Figure 3. Variations in real WOB and ROP with different nominal WOB. (a) Real WOB; (b) ROP.

Even though under a certain nominal WOB, the load transfer efficiency decreases in a well with a longer horizontal section and higher friction coefficients. As can be

seen in Figures 4 and 5, the amplitude of the downhole WOB fluctuation increases and the frequency decreases with the increase in the horizontal section length and friction coefficients when the nominal WOB equals 100 kN, which means that the load transfer becomes worse.



**Figure 4.** The effect of horizontal section length on WOB.

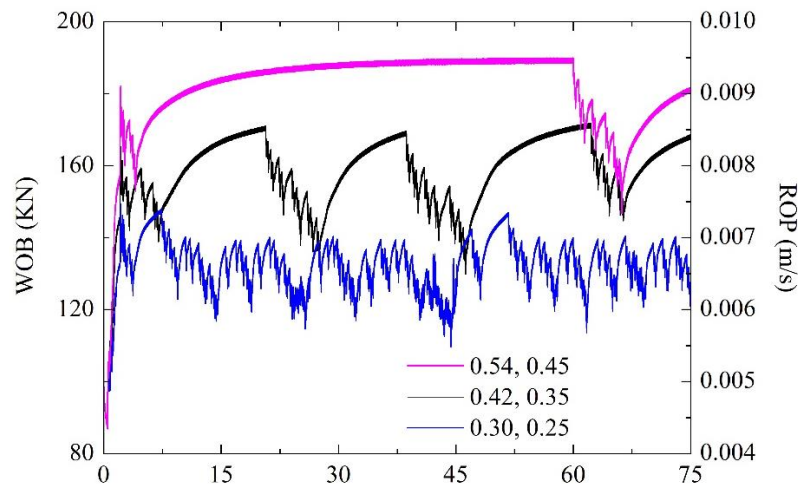


**Figure 5.** The effect of friction coefficients on WOB and ROP.

As can be seen from Figure 3, the WOB fluctuates severely under a lower WOB, and the drill-string cannot move continuously under 60 kN WOB. The reason for this is the stick-slip phenomenon of the drill-string caused by the static-dynamic friction switch between the drill-string and the borehole wall. If we apply an axial exciting force with an amplitude of 20 kN and a frequency of 10 Hz on the drill-string at the surface, will the load transfer be improved? Figure 6 shows the WOB changes during typical slide drilling and surface vibration drilling. From Figure 6, the real WOB and ROP improve significantly after applying vibration at the surface, and the WOB curve becomes smoother, which is beneficial for the drilling operation.

### 3.2. Influence Factor Analysis

According to the analysis of Section 3.1, we know that the real WOB and ROP improve significantly after applying vibration at the surface, which means that the drill-string axial vibration at the surface technology is effective. However, the questions as to whether it is efficient and how to set the vibrating parameters should be answered. In the application process of this technology, we can only adjust the amplitude and the frequency of the

exciting force to control the effectiveness of load transfer. Figure 7 shows the influences of the amplitude and the frequency of the exciting forces on the WOB and ROP. As can be seen from Figure 7, the WOB becomes smooth and fluctuates less with the increase in the amplitude or frequency of the exciting force. The stick–slip phenomenon is suppressed significantly. The WOB and ROP are sensitive to the exciting frequency at a low exciting amplitude, but they are rarely affected at a larger exciting force. Therefore, better load transfer results can be obtained at a higher exciting force amplitude even though the exciting frequency changes a lot in drilling.

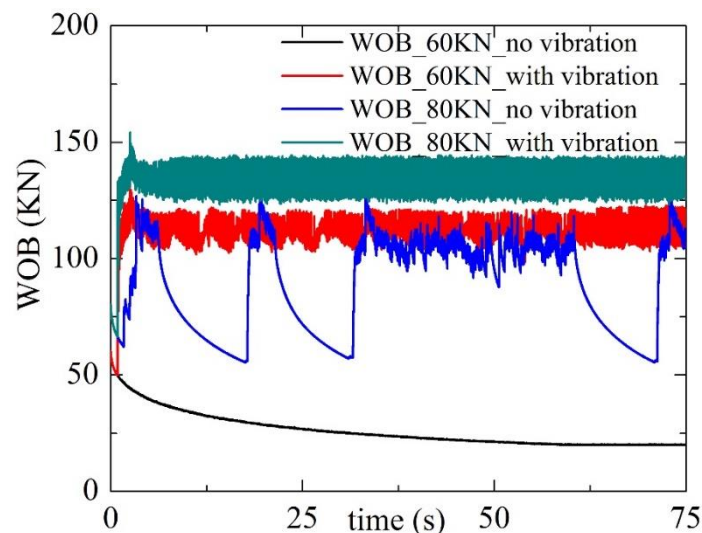


**Figure 6.** WOB changes during surface vibration drilling.

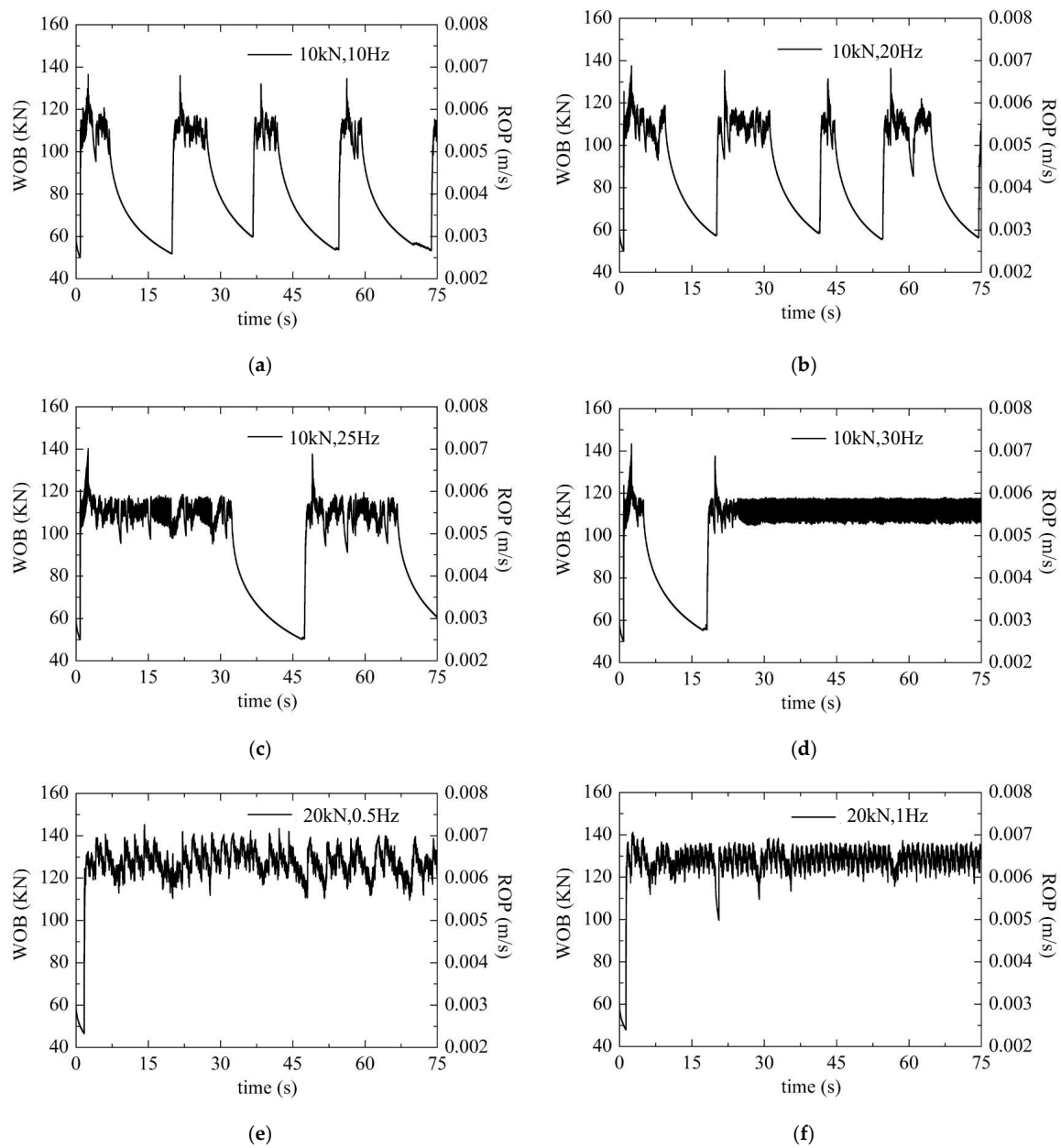
### 3.3. Safety Evaluation of Surface Vibrated Drill-String

The introduction of vibration in drilling can reduce the friction between the drill-string and the wellbore wall and improve the load transfer efficiency, and a higher exciting amplitude or frequency is good for improving friction reduction and load transfer effectiveness. However, vibration of the drill-string will simultaneously increase the internal stress and the failure risk of the drill-string. Therefore, the increase in the exciting amplitude and frequency must be restricted by the dynamic safety of the drill-string. The methods for evaluating the drill-string's safety mainly include the safety factor method and the real-time monitoring of downhole tools. Drill stem design and operation [32] indicates that overload or fatigue are the two main reasons for drill-string failure. In the process of drill-string design, the safety factors in the stretch and torsional direction are 1.0 to 1.3, which guarantee the real stress of the drill-string is lower than the allowable stress.

However, the safety factor method does not consider the effect of induced vibration on drill-string safety. A large number of statistical results of drill-string failure indicate that drill-string vibration will result in a dramatic change in the drill-string stress on the premise that the drill-string stress is lower than the allowable stress, which will influence the safety of the drill-string. Based on the above considerations, several petroleum technology service corporations have developed underground vibration monitoring systems (such as the VSS system of Baker Hughes, MVC system of Schlumberger, and TVM system of Weatherford; the installation methods of these systems are different) to control the vibration and decrease the dynamic stress level of the drill-string by adjusting the drilling parameters in the drilling process. We adopted the method of Baker Hughes (see Table 1 [33]) to evaluate the safety of the drill-string axial vibration at the surface technology proposed in this paper.

**Table 1.** Vibration level classification (Baker Hughes INTEQ company).

| Grade | Vibration Level in Axial Direction RMS(g) | Color Marking | Evaluation Result |
|-------|---|---------------|-------------------|
| 0     | [0.0, 0.5)                                | green         | safe              |
| 1     | [0.5, 1.0)                                |               |                   |
| 2     | [1.0, 2.0)                                | yellow        | caution           |
| 3     | [2.0, 3.0)                                |               |                   |
| 4     | [3.0, 5.0)                                | red           | danger            |
| 5     | [5.0, 8.0)                                |               |                   |
| 6     | [8.0, 15.0)                               |               |                   |
| 7     | [15.0, $\infty$ )                         |               |                   |

**Figure 7.** Cont.

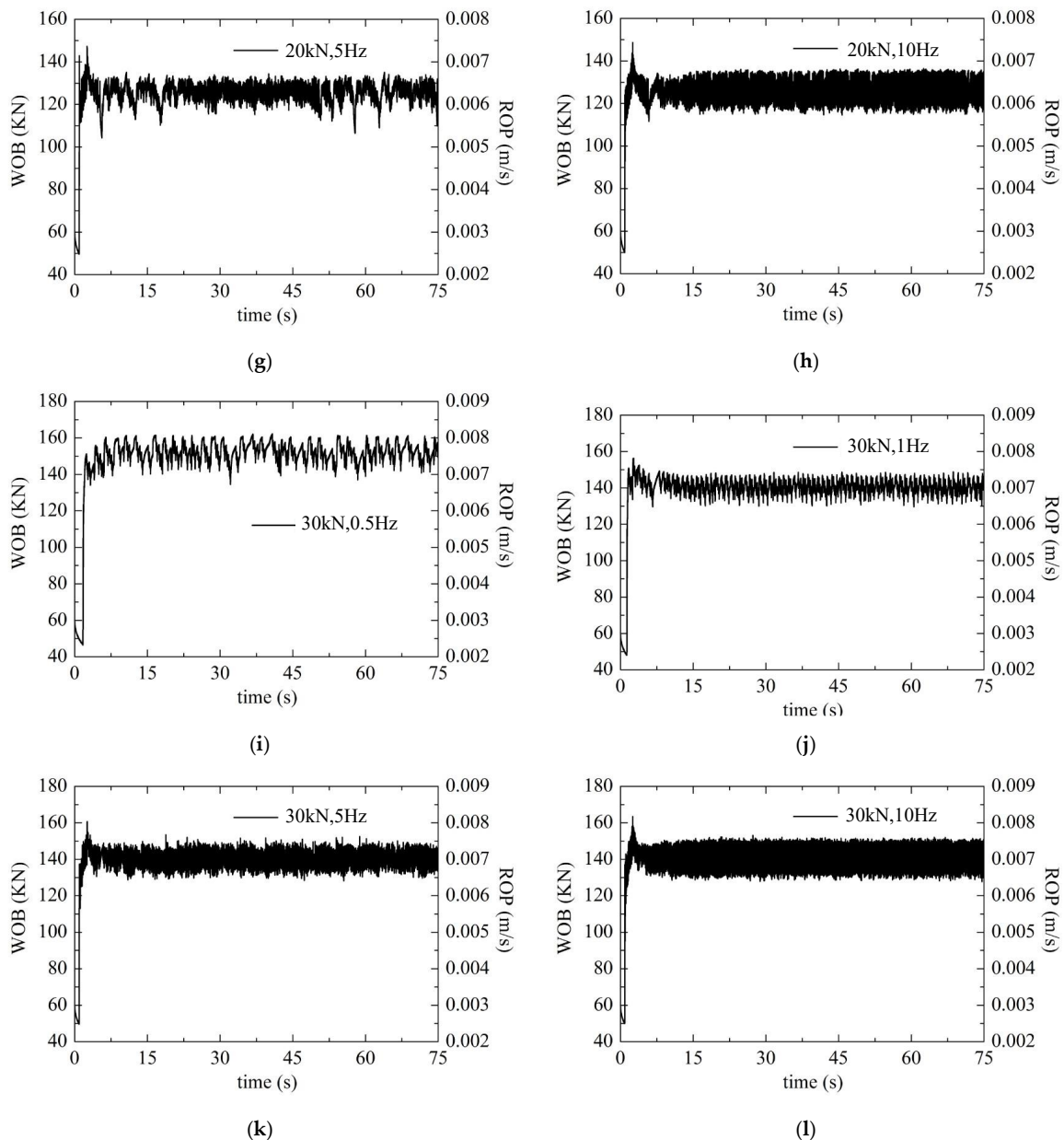


**Figure 7.** WOB and ROP under different exciting forces. (a) 10 kN, 10 Hz. (b) 10 kN, 20 Hz. (c) 10 kN, 25 Hz. (d) 10 kN, 30 Hz. (e) 20 kN, 0.5 Hz. (f) 20 kN, 1 Hz. (g) 20 kN, 5 Hz. (h) 20 kN, 10 Hz. (i) 30 kN, 0.5 Hz. (j) 30 kN, 1 Hz. (k) 30 kN, 5 Hz. (l) 30 kN, 10 Hz.

Figure 8 shows the maximal and root mean square (RMS) acceleration along the drill-string. As can be seen from Figure 8, the maximal and RMS acceleration generally show a trend of increasing with the increase in the exciting force amplitude and frequency. According to the change in drill-string acceleration, the whole drill-string can be divided into three segments by the kickoff point (depth = 1290 m) and landing point (depth = 2190 m). In the case that the exciting force amplitude equals 10 kN, the maximal acceleration of the building up section and the horizontal section is larger than that of the vertical section, while the RMS acceleration is close. The maximal acceleration and RMS acceleration show a lower value under 10 Hz and 30 Hz. From Figure 7, we can see the load transfer under 10–25 Hz is far from 30 Hz. Therefore, a higher frequency should be applied in order to obtain a better load transfer effect and lower acceleration. In the case that the exciting force amplitude equals 20 kN and 30 kN, the maximal acceleration of the building up section and the horizontal section is larger than that of the vertical section, while the RMS acceleration shows the opposite trend. For maximal

acceleration, a lower value is obtained at 5 Hz and 10 Hz and the highest value is obtained at 0.5 Hz in the vertical section, while a lower value is obtained at 10 Hz to 30 Hz and the highest value is obtained at 0.5 Hz to 5 Hz in the horizontal section. For RMS acceleration, a lower value is obtained at 0.5 Hz to 5 Hz and the highest value is obtained at 20 Hz to 30 Hz in the vertical section, while a lower value is obtained at 10 Hz to 30 Hz and the highest value is obtained at 0.5 Hz to 5 Hz in the horizontal well section. Therefore, we can see that the RMS acceleration shows an opposite trend in the vertical and horizontal sections. When the frequency equals 10 Hz, the differences in the RMS between the different well sections are small and the RMS acceleration of the whole drill-string has a lower value. Therefore, 10 Hz is the optimum value for drill-string safety under the conditions set by the given parameters.

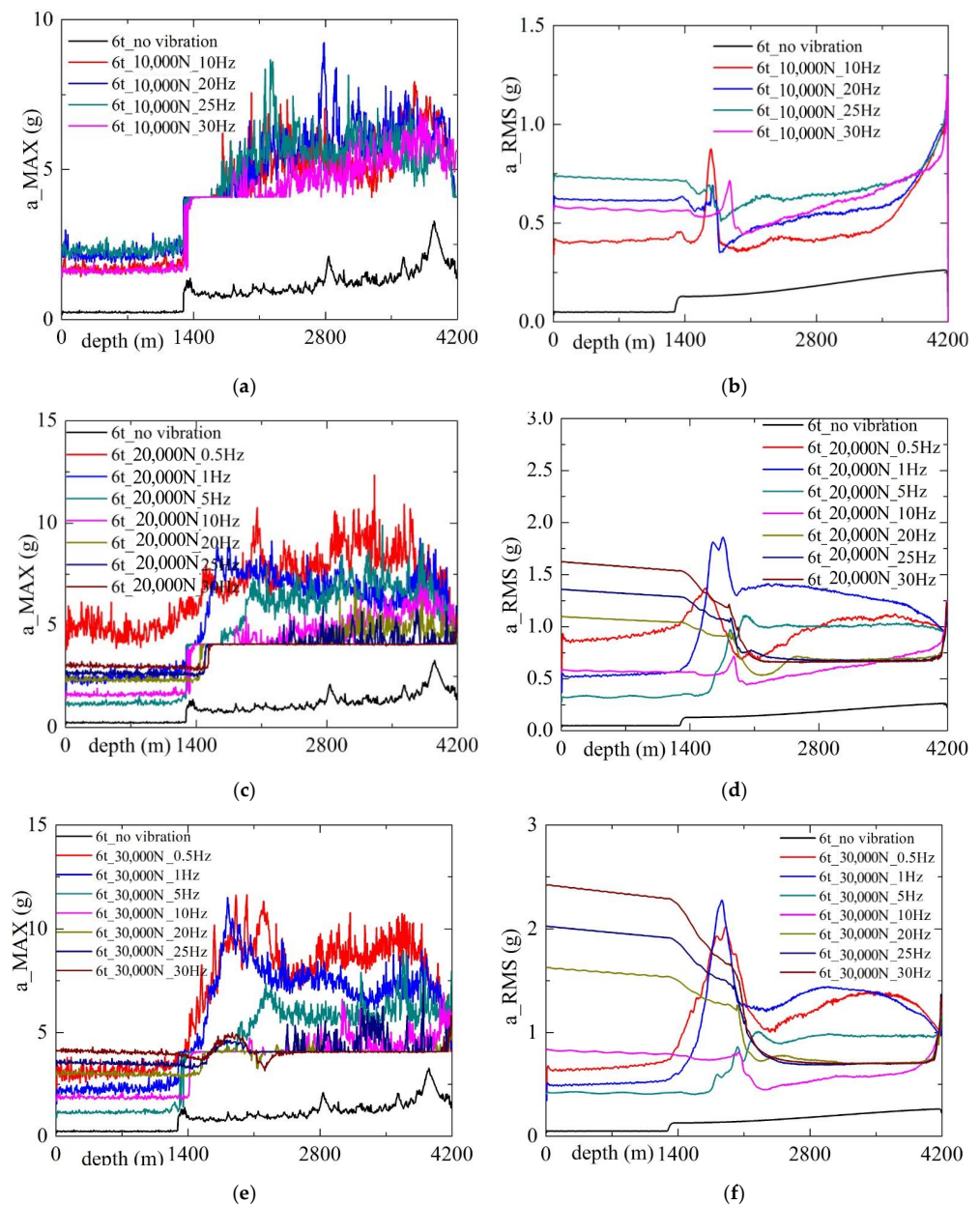


**Figure 8.** Maximal and root mean square acceleration along the drill-string under different exciting force amplitude. (a) Max: 10 kN. (b) RMS: 10 kN. (c) Max: 20 kN. (d) RMS: 20 kN. (e) Max: 30 kN. (f) RMS: 30 kN.

According to the vibration level classification method shown in Table 1, the safety grades along the drill-string under different exciting parameters are shown in Table 2. From Table 2, the

drill-string near bit is all in the caution (two grade) state, which means that its RMS acceleration ranges from 1 g to 2 g. Only when the amplitude of the exciting force equals 30 kN and the frequency is lower than 1 Hz or more than 25 Hz, is it certain that the well section is in the caution (three grade) state, which means that its RMS acceleration ranges from 2 g to 3 g. Caution (two grade) should be avoided, and caution (three grade) is dangerous for longstanding drilling. According to Table 2, 5 Hz to 10 Hz is the optimum frequency range for drill-string axial vibration at the surface technology under the given parameters.

**Table 2.** Safety evaluation results of drill-string while being axially vibrated at surface.

| Frequency/Hz<br>Exciting Force/kN |        | 0                    | 0.5                 | 1      | 5                      | 10     | 20                       | 25     | 30     |
|-----------------------------------|--------|----------------------|---------------------|--------|------------------------|--------|--------------------------|--------|--------|
|                                   |        | 100                  | 0~4200              |        |                        |        |                          | 0~1600 | 0~1750 |
|                                   |        |                      |                     |        |                        | ~1750  | ~2450                    | ~4200  | ~2330  |
|                                   |        |                      |                     |        |                        | ~3530  | ~4150                    |        | ~4170  |
|                                   |        |                      |                     |        |                        | ~4170  | ~4200                    |        | ~4200  |
| 200                               | 0~4200 |                      | 0~1230              | 0~1520 | 0~1660                 | 0~1920 | 0~1415                   | 0~1865 | 0~1895 |
|                                   |        |                      | ~1755               | ~4110  | ~1940                  | ~2330  | ~4180                    | ~4180  | ~4180  |
|                                   |        |                      | ~2780               | ~4180  | ~3970                  | ~4170  | ~4200                    | ~4200  | ~4200  |
|                                   |        |                      | ~4095               | ~4200  | ~4175                  | ~4200  |                          |        |        |
|                                   |        |                      | ~4180               |        | ~4200                  |        |                          |        |        |
| 300                               | 0~4200 |                      | 0~1455              | 0~555  | 0~1775                 | 0~2210 | 0~2075                   | 0~275  | 0~1570 |
|                                   |        |                      | ~1890               | ~1620  | ~2220                  | ~2555  | ~4175                    | ~2130  | ~2155  |
|                                   |        |                      | ~1915               | ~1790  | ~2285                  | ~4160  | ~4200                    | ~4165  | ~4165  |
|                                   |        |                      | ~4200               | ~1915  | ~4160                  | ~4200  |                          | ~4200  | ~4200  |
|                                   |        |                      |                     | ~4200  | ~4200                  |        |                          |        |        |
|                                   |        | Safe<br>(zero grade) | Safe<br>(one grade) |        | Caution<br>(two grade) |        | Caution<br>(three grade) |        |        |

**4. Conclusions**

This work proposed a method to reduce friction and improve the ROP of slide drilling. The method applies axial vibration on the drill-string at the surface. A mathematical vibration model was established to simulate the load transfer in the drill-string, and this paper discussed the advantages, influencing factors, and feasibility of the drill-string axial vibration at the surface technology.

Numerical modeling results show that the motion of the drill-string in the conventional drilling process has stick-slip features, and the WOB is fluctuant with certain frequencies. If the friction force equals the weight of the upper drilling string, no weight can be transmitted to the bit. The conventional method of calibrating the WOB using a weight indicator gauge is not suitable when the ROP is slow. The proposed technology of applying axial vibration to the drill-string at the surface has been proven to be highly effective. This is supported by the significant increase in the WOB resulting from the release of friction after the application of the vibration. The amplitude and frequency of the exciting forces are the main influence factors of the effectiveness of the application of this technology and the safety of the drill-string. The horizontal well section exhibits a high RMS acceleration at low frequencies, whereas the vertical well section demonstrates a high RMS acceleration at high frequencies. There is an optimal frequency for a given case (10 Hz in this paper). This means that the conventional manual pick-up and slack-off at the surface with a high amplitude and low frequency has little friction reduction effect. Safety evaluation results indicate that the drill-string is in a safe state under most of the exciting parameters.

Some simplification and issues should be considered in future research, such as:

(a) Utilizing the soft-string model in the mathematical model accommodates accurate results for wells with less curvature on site. However, it may lead to significant discrepancies in high curvature intervals.

(b) During the drilling process, the drill-string is composed of joints and centralizers. The borehole wall is not uniform in shape and the gap between the drill-string and the borehole wall cannot be disregarded. These factors will inevitably impact the principles of friction reduction and load transfer. Therefore, the actual conditions should be considered in future research.

**Author Contributions:** Y.L. conceived and designed the program, and X.W. supervised the study and debugged the program. P.W. assisted in the development of the algorithm. F.Z. analyzed the computed results and wrote the paper. All authors have read and agreed to the published version of the manuscript.

**Funding:** This paper is sponsored by the Hubei Key Laboratory of Oil and Gas Drilling and Production Engineering (Yangtze University) (Grant No. YQZC202208) (X.W.), and Hubei Provincial Science and Technology Agency (Grant No. 2019CFA093) (Z.F.).

**Data Availability Statement:** The data used to support the findings of this study are available from the corresponding author upon request.

**Acknowledgments:** The authors also gratefully acknowledge the financial support of the CNPC Bohai Drilling Corporation.

**Conflicts of Interest:** The authors declare no conflict of interest.

## Nomenclature

Roman symbols:

|                                   |   |
|-----------------------------------|---|
| $a, b$                            | weight on bit exponent and rotate speed exponent, respectively                              |
| $A$                               | cross-section area of drill-string, $m^2$   |
| $c$                               | drilling fluid drag, $N\ s/m^2$   |
| $D$                               | inner diameter of drill-string, m   |
| $E$                               | Elastic (Young's) modulus of drill-string, Pa   |
| $\vec{e}_g$                       | vector of submerged drill-string weight   |
| $\vec{e}_t, \vec{e}_n, \vec{e}_b$ | unit base vectors in natural curvilinear system   |
| $f$                               | frequency of vibration, Hz  |
| $F, F_n, F_b$                     | normal contact force and its components in $\vec{e}_n$ and $\vec{e}_b$ direction, N         |
| $F_c$                             | Coulomb friction force, N   |
| $F_a$                             | amplitude of exciting force, N  |
| $F_f$                             | axial friction force, N   |
| $F_{f,s}$                         | total static friction of drill-string, N  |
| $F_{top}$                         | hook load, N  |
| $g_s$                             | linear buoyant weight of drill-string, N/m  |
| $g(x)$                            | constraint condition  |
| $G_t$                             | axial component of gravity of the whole drill-string, N                                     |
| $h$                               | space step, m   |
| $i$                               | parameter determines the shape of strain–stress curve                                       |
| $k_\alpha$                        | rate of change of deviation angle, and, respectively, rad/m                                 |
| $k_\varphi$                       | rate of change of azimuth angle, rad/m  |
| $k_b$                             | total bending curvature, rad/m  |
| $K_t$                             | tangential stiffness of contact surfaces, N/m   |
| $L$                               | length of drill-string, m   |
| $n$                               | rotate speed of drill-string, $2\pi$ rad/s  |
| $ROP$                             | rate of penetration, m/s  |
| $s$                               | well depth, m   |
| $t$                               | time, s   |
| $T_{max}$                         | strength of drill-string, N   |
| $T, T_t, T_n, T_b$                | internal tension force and its components in $\vec{e}_t, \vec{e}_n, \vec{e}_b$ direction, N |
| $u$                               | axial displacement of drill-string, m   |
| $v_r$                             | relative velocity of drill-string, m/s  |
| $WOB$                             | weight on bit, N  |
| $z(t)$                            | offset displacement of asperities at time $t$ , m   |

## Greek symbols:

|                |   |
|----------------|---|
| $\alpha$       | deviation angle, rad  |
| $\varphi$      | azimuth angle, rad  |
| $\tau$         | time step, s  |
| $\Phi$         | initial displacement distribution of drill-string, m        |
| $\bar{\alpha}$ | mean deviation angle, rad                                   |
| $\rho$         | density of drill-string, kg/m <sup>3</sup>                  |
| $\mu$          | instantaneous friction coefficient in $\vec{e}_t$ direction |
| $\mu_s$        | static friction coefficient                                 |
| $\mu_d$        | dynamic friction coefficient                                |
| $\omega$       | circular frequency of the excitation, Hz                    |

## References

- Gao, D.; Tan, C.; Tang, H. Limit analysis of extended reach drilling in South China Sea. *Pet. Sci.* **2009**, *6*, 166–171. [[CrossRef](#)]
- Roper, W.F.; Dellinger, T.B. Reduction of the Frictional Coefficient in a Borehole by the Use of Vibration. US Patent 4384625, 24 May 1983.
- Maidla, E.; Haci, M.; Jones, S.; Cluchey, M.; Alexander, M.; Warren, T. Field Proof of the New Sliding Technology for Directional Drilling. In Proceedings of the SPE/IADC Drilling Conference, Amsterdam, The Netherlands, 23–25 February 2005.
- Jones, S.; Feddema, C.; Sugiura, J.; Lightey, J. A New Friction Reduction Tool with Axial Oscillation Increases Drilling Performance: Field-Testing with Multiple Vibration Sensors in One Drill String. In Proceedings of the IADC/SPE Drilling Conference and Exhibition, Fort Worth, TX, USA, 1–3 March 2016.
- Ali, A.A.; Barton, S.; Mohanna, A. Unique axial oscillation tool enhances performance of directional tools in extended reach applications. In Proceedings of the Brasil Offshore Conference and Exhibition, Macae, Brazil, 14–17 June 2011.
- Skyles, L.; Amiraslani, Y.; Wilhoit, J. Converting Static Friction to Kinetic Friction to Drill Further and Faster in Directional Holes. In Proceedings of the IADC/SPE Drilling Conference and Exhibition, San Diego, CA, USA, 6–8 March 2012.
- Gee, R.; Hanley, C.; Hussain, R.; Canuel, L.; Martinez, J. Axial Oscillation Tool vs. Lateral Vibration Tools for Friction Reduction—What’s the Best Way to Shake the Pipe? In Proceedings of the SPE/IADC Drilling Conference and Exhibition, London, UK, 17–19 March 2015.
- Eric, M.; Marc, H.; Daniel, W. Case history summary: Horizontal drilling performance improvement due to torque rocking on 800 horizontal land wells drilled for unconventional gas resources. In Proceedings of the SPE Annual Technical Conference and Exhibition, New Orleans, Louisiana, 4–7 October 2009.
- Gillan, C.; Boone, S.; Kostiuik, G.; Schlembach, C.; Pinto, J.; LeBlanc, M. Applying precision drill pipe rotation and oscillation to slide drilling problems. In Proceedings of the SPE/IADC Drilling Conference, Amsterdam, The Netherlands, 17–19 March 2009.
- Sheppard, M.C.; Wick, C.; Burgess, T. Designing well paths to reduce drag and torque. *SPE Drill. Eng. New Orleans* **1987**, *2*, 344–350. [[CrossRef](#)]
- Maidla, E.E.; Wojtanowicz, A.K. Field Comparison of 2D and 3D Methods for the Borehole Friction Evaluation in Directional Wells. In Proceedings of the 62nd Annual Technical Conference and Exhibition, Dallas, TX, USA, 27–30 September 1987.
- Paslay, P.R. Stress Analysis of Drillstrings. In Proceedings of the University of Tulsa Centennial Petroleum Engineering Symposium, Tulsa, Oklahoma, 29–31 August 1994.
- Aadnoy, B.S.; Andersen, K. Design of oil wells using analytical friction models. *J. Pet. Sci. Eng.* **2001**, *32*, 53–71. [[CrossRef](#)]
- Johancsik, C.A.; Friesen, D.B.; Dawson, R. Torque and drag in directional wells—prediction and measurement. *J. Pet. Technol.* **1984**, *36*, 987–992. [[CrossRef](#)]
- Ho, H.S. An Improved Modeling Program for Computing the Torque and Drag in Directional and Deep Wells. In Proceedings of the SPE Annual Technical Conference and Exhibition, Houston, TX, USA, 2–5 October 1988.
- Adewuya, O.A.; Pham, S.V. A robust torque and drag analysis approach for well planning and drillstring design. *J. Pet. Technol.* **1998**, *50*, 1–16.
- Rezmer-Cooper, I.; Chau, M.; Hendricks, A.; Woodfine, M.; Stacey, B.; Downton, N. Field Data Supports the Use of Stiffness and Tortuosity in Solving Complex Well Design Problems. In Proceedings of the IADC/SPE Drilling Conference, Amsterdam, Holland, 9–11 March 1999. IADC/SPE 52819.
- Zifeng, L.; Xisheng, L.; Daqian, Z. A Steady Tension-torque Model for Drillstring in Horizontal Wells. *Pet. Drill. Technol.* **1993**, *20*, 1–6.
- Dykstra. *Nonlinear Drill String Dynamics*; University of Tulsa: Tulsa, OK, USA, 1996.
- Pabon, J.; Wicks, N.; Chang, Y.; Dow, B.; Harmer, R. Modeling Transient Vibrations While Drilling Using a Finite Rigid Body Approach. In Proceedings of the SPE Deepwater Drilling and Completions Conference, Galveston, TX, USA, 5–6 October 2010.
- Wicks, N.; Pabon, J.; Auzeais, F.; Kats, R.; Godfrey, M.; Chang, Y.; Zheng, A. Modeling of Axial Vibrations to Allow Intervention in Extended Reach Wells. In Proceedings of the SPE Deepwater Drilling and Completions Conference, Galveston, TX, USA, 20–21 June 2012.
- Ritto, T.G.; Escalante, M.R.; Rosales, M.B. Drill-string horizontal dynamics with uncertainty on the frictional force. *J. Sound Vib.* **2013**, *332*, 145–153. [[CrossRef](#)]
- Wang, X.M.; Chen, P.; Ma, T.S.; Liu, Y. Modeling and experimental investigations on the drag reduction performance of an axial oscillation tool. *J. Nat. Gas Sci. Eng.* **2017**, *39*, 118–132. [[CrossRef](#)]

24. Wang, P.; Ni, H.; Wang, R. Experimental investigation of the effect of in-plane vibrations on friction for different materials. *Tribol. Int.* **2016**, *99*, 237–247. [[CrossRef](#)]
25. Gutowski, P.; Leus, M. The effect of longitudinal tangential vibrations on friction and driving forces in sliding motion. *Tribol. Int.* **2012**, *55*, 108–118. [[CrossRef](#)]
26. Gutowski, P.; Leus, M. Computational model for friction force estimation in sliding motion at transverse tangential vibrations of elastic contact support. *Tribol. Int.* **2015**, *90*, 455–462. [[CrossRef](#)]
27. Tolstoi, D.M.; Borisova, G.A.; Grigorova, S.R. Friction regulation by perpendicular oscillation. *Sov. Phys. Dokl.* **1973**, *17*, 80–86.
28. Gao, B.K.; Gao, D.L. Possibility of drill stem buckling in inclined hole. *Oil Drill. Prod. Technol.* **1995**, *17*, 6–11.
29. Wang, P.; Ni, H.J.; Wang, X.Y.; Wang, R.; Lu, S. Research on the characteristics of earthworm-like vibration drilling. *J. Pet. Sci. Eng.* **2018**, *160*, 60–71. [[CrossRef](#)]
30. Dahl, P.R. Solid friction damping of mechanical vibrations. *AIAA J.* **1976**, *14*, 1675–1682. [[CrossRef](#)]
31. Yan, T. *Theory and Practice of Optimizing Drilling Parameters*; Harbin Institute of Technology Press: Harbin, China, 1994.
32. TH HILL. *Standard DS-1: Drill Stem Design and Operation*; TH HILL Associates: Houston, TX, USA, 2004.
33. Hu, Y.B.; Di, Q.F.; Zou, H.Y. The New Developments of Monitoring Technology and Researches on Drill String Dynamics. *Petroleum Drill. Technol.* **2006**, *34*, 7–10.

**Disclaimer/Publisher’s Note:** The statements, opinions and data contained in all publications are solely those of the individual author(s) and contributor(s) and not of MDPI and/or the editor(s). MDPI and/or the editor(s) disclaim responsibility for any injury to people or property resulting from any ideas, methods, instructions or products referred to in the content.